Fragmentation of α- and β-alanine molecules by ions at Bragg-peak energies

Bari, S.; Sobocinski, P.; Postma, J.; Alvarado, F.; Hoekstra, R.; Bernigaud, V.; Manil, B.; Rangama, J.; Huber, B.; Schlathoelter, T.

Published in:
Journal of Chemical Physics

DOI:
10.1063/1.2830032

Publication date:
2008

Fragmentation of α- and β-alanine molecules by ions at Bragg-peak energies

S. Bari, P. Sobocinski, J. Postma, F. Alvarado, R. Hoekstra, V. Bernigaud, B. Manil, J. Rangama, B. Huber, and T. Schlathölter

Citation: The Journal of Chemical Physics **128**, 074306 (2008); doi: 10.1063/1.2830032
View online: https://doi.org/10.1063/1.2830032
View Table of Contents: http://aip.scitation.org/toc/jcp/128/7
Published by the American Institute of Physics

Fragmentation of α- and β-alanine molecules by ions at Bragg-peak energies

S. Bari,[1] P. Sobocinski,[1] J. Postma,[1] F. Alvarado,[1] R. Hoekstra,[1] V. Bernigaud,[2] B. Manil,[2] J. Rangama,[2] B. Huber,[2] and T. Schlathölter[1,a)]
[1]*KVI Atomic Physics, University of Groningen, Zernikelaan 25, 9747AA Groningen, The Netherlands*
[2]*Centre Interdisciplinaire de Recherches Ions Lasers (CIRIL), CEA-CNRS-ENSICAEN-UCBN, Bd. Henri Becquerel, BP 5133, F-14070 Caen Cedex 05, France*

(Received 25 September 2007; accepted 6 December 2007; published online 20 February 2008)

The interaction of keV He^+, He^{2+}, and O^{5+} ions with isolated α and β isomers of the amino acid alanine was studied by means of high resolution coincidence time-of-flight mass spectrometry. We observed a strong isomer dependence of characteristic fragmentation channels which manifests in strongly altered branching ratios. Despite the ultrashort initial perturbation by the incoming ion, evidence for molecular rearrangement leading to the formation of H_3^+ was found. The measured kinetic energies of ionic alanine fragments can be sufficient to induce secondary damage to DNA in a biological environment. © *2008 American Institute of Physics*. [DOI: 10.1063/1.2830032]

INTRODUCTION

Biological effects of ionizing radiation are known to be mainly due to direct or indirect damage of cellular DNA. To understand biological radiation damage on a molecular level, a number of recent studies have focused on the ionization and fragmentation of isolated DNA building blocks. It was, for instance, found that very low energy (secondary) electrons can efficiently damage nucleobases[1–3] or deoxyribose[4] and eventually lead to DNA single and double strand breaks.[5–7] The interaction of keV ions with DNA is of major biological relevance in the context of the recent advances in proton and heavy ion tumor therapy. When the ions are decelerated to sub-MeV energies, the so-called Bragg peak is reached where the induced damage is maximum. It has been observed that nucleobases[8–12] and even more so deoxyribose molecules[13] are very sensitive to keV ion impact. Furthermore, secondary ions produced in such collisions can have kinetic energies easily exceeding 10 eV,[9,10] which is sufficient to cause subsequent DNA damage.[14,15]

In the nuclei of eukaryotic cells, DNA is wound around protein spools—the so-called histones. The radiation action upon these proteins is of interest since secondary particles formed during the interaction might in turn damage the neighboring DNA. We have studied the singly and multiply charged ion (MCI) induced ionization and fragmentation of a common protein building block, the amino acid alanine. Collisions are studied at keV (Bragg peak) projectile energies with emphasis on the determination of secondary ion energies.

Alanine $[CH_3–CH(NH_2)–COOH]$ is the only amino acid which naturally occurs in two different isomers (α- and β-alanine). The two alanine isomers are depicted in Fig. 1 with the molecular structure of their lowest energy gas-phase conformer, as experimentally identified by Alonso and co-workers.[16,17] This availability of two stable isomers allowed us to also address the fundamental question whether there is a structural sensitivity of biomolecular fragmentation pathways following collisions with multiply charged ions. It is known, e.g., from MCI collisions with C_{60} that electron capture at large impact parameters can be a very gentle ionization process accompanied by only small amounts of target excitation.[18,19] Distinct isomer effects in the ionization and fragmentation dynamics following MCI interactions with alanine would indicate that fragmentation patterns might also contain structural information for other amino acids and possibly even for peptides or proteins. This could ultimately be interesting for the potential application of keV MCI impact as a tool for protein sequencing.

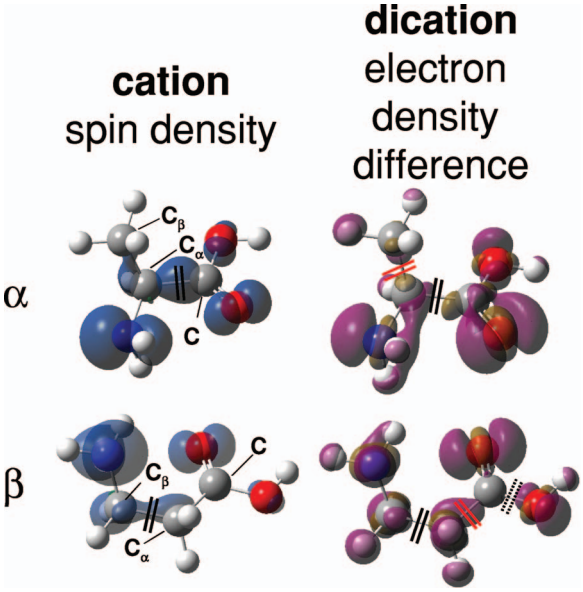

FIG. 1. (Color) Molecular structure of α- (top) and β-alanine (bottom, dark gray: O; gray: N; light gray: C; white: H). In the left column, the spin density of the cationic molecule is indicated as the shaded area; in the right column, the electron density difference map of the dication with respect to the cation is displayed. The double lines indicate bond scission, leading to the dominating fragments.

a)Electronic mail: tschlat@kvi.nl.

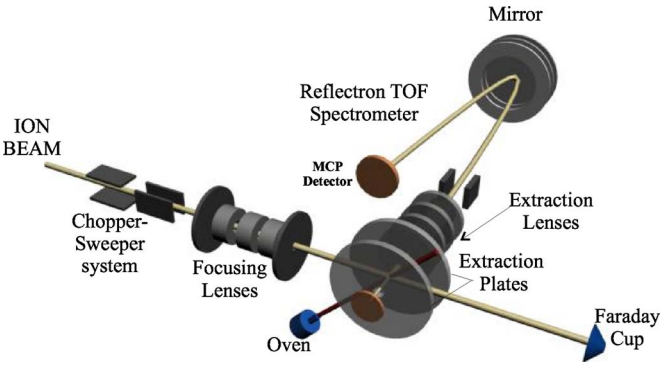

FIG. 2. (Color online) Sketch of the experimental setup.

In addition, very recently, De *et al.* observed H_3^+ formation in collisions of keV Ar^{8+} ions with methanol molecules[20]—a process which is important, e.g., for interstellar gas-phase chemistry. The H_3^+ could only be formed via fast bond rearrangement following Franck-Condon-type double ionization processes. In this paper, we show that H_3^+ formation following MCI collisions is not limited to methanol but also occurs in both α- and β-alanine and thus seems to be a more general phenomenon.

EXPERIMENT

The experimental setup has been described in detail previously.[8] A sketch is displayed in Fig. 2. Briefly, He^+, He^{2+}, and O^{5+} ions were extracted from the electron cyclotron resonance ion source located at the ZernikeLEIF facility (KVI in Groningen).

For the present experiments, the source was operated on potentials between 4 and 20 kV. The ion beam was pulsed with a repetition rate in the 10 kHz range and an ion-pulse length of about 10 ns. In the setup, the ion beam was collimated by means of two 1 mm diaphragms (205 mm apart) and focused into the collision region.

In the collision chamber, the ion-beam pulses crossed a gaseous target of α- or β-alanine, evaporated from an oven resistively heated to 420 K. This temperature ensured sufficient target densities without thermal dissociation of the molecules. The molecules then effused through a 500 μm nozzle placed $\approx$20 mm from the collision region. A liquid nitrogen cooled stainless steel plate opposite to the oven nozzle serves as a trap for the alanine as well as residual gas components. This way the base pressure during experiments is kept around 1×10^{-8} mbar and contributions of the residual gas to the experimental data are negligible.

Two extraction plates located 10 mm apart provide a static electric field. For most experiments, an electric field of 150 V/cm was used. To avoid coverage of these plates by adsorbed layers of alanine, which would distort the homogeneous field, both plates were resistively heated to $\approx$100 °C. Due to the electric field, ions generated in the collision region were extracted through a diaphragm and a lens system into a reflectron time-of-flight (TOF) spectrometer [resolution $m/\Delta m=1500$ at $m=720$ amu (Ref. 21)] and detected on a multichannel-plate detector. The signal sent to the ion-beam pulser was used as a start for the TOF measurement

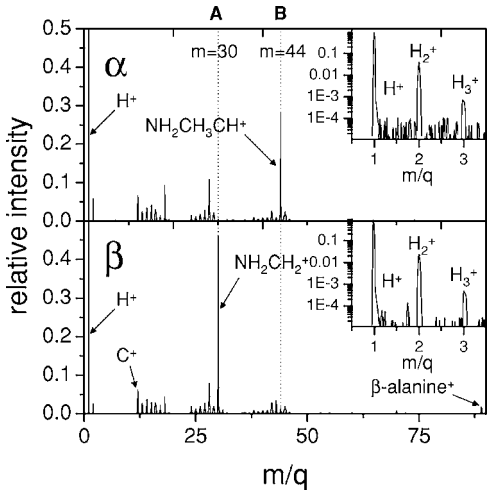

FIG. 3. Mass spectrum of product ions from 40 keV He^{2+} collisions with α-alanine (top) and β-alanine (bottom). A and B label the main interaction products $NH_2CH_2^+$ and $NH_2CH_3CH^+$, formed by cleavage of the C–C_α bond (α-alanine) and of the C_α–C_β bond (β-alanine), respectively.

and for each start, several fragment ions could be detected in coincidence (dead time $\approx$50 ns) and analyzed in an event-by-event mode. Electronically, this was accomplished by using a multihit time-to-digital converter (FAST 7888, 1 ns resolution).

RESULTS AND DISCUSSION

A typical mass spectrum of positively charged products from collisions of 40 keV He^{2+} with the two alanine isomers is shown in Fig. 3. For α-alanine, the probability of nondissociative ionization is negligible, but also for β-alanine, the contribution of the parent cation is weak. For both isomers, the fragmentation spectra are particularly rich and for α-alanine, a qualitative resemblence with data obtained after low energy electron impact[22] and core excitation[23] is obvious. A list with the yields of the most dominant α-alanine fragments and their tentative assignment can be found in Table I. Data for He^+ and O^{5+} are given for comparison.

One issue to address here is the formation of H_3^+ fragment ions. This process has been observed recently for MCI induced double ionization of CH_3OH and the H_3^+ was confirmed to exclusively stem from the methyl group.[20] We observe H_3^+ formation as a weak channel in all collision systems (see inset in Fig. 3), being strongest for 50 keV O^{5+} projectiles (α-alanine: 0.1% of the H^+ ion yield; β-alanine: 0.05%) and about a factor of 2 smaller for 10 keV He^+ and He^{2+} at different kinetic energies. β-alanine does not have a CH_3 group and H_3^+ formation, therefore, requires proton migration. α-alanine, on the other hand, has a CH_3 sidechain. H_3^+ formation in this case does not necessarily require proton migration. However, when using α-alanine with a fully deuterated sidechain, we observed about twice as much D_2H^+ as D_3^+. Also for α-alanine, the trihydrogen cation is, therefore, primarily formed in a process requiring proton migration.

For α-alanine, the dominant fragment cations are found at $m/q=1$ (H^+) and at $m/q=44$ ($NH_2CH_3CH^+$, referred to as B in Fig. 3). The latter fragment is formed by a single rupture of the C–C_α bond indicated in Fig. 1. *Ab initio* calculations

TABLE I. Relative yields of the dominant cationic fragments (yield: 0.1% or more with the exception of H_3^+) of α-alanine formed in collisions with 10 keV He^+, 20 keV He^{2+}, and 50 keV O^{5+}.

m/q (amu)	Ion assignment	He^+ (%)	He^{2+} (%)	O^{5+} (%)
1	H^+	32.4	41.9	44.8
2	H_2^+	1.7	0.6	1.6
3	H_3^+	0.07	0.02	0.9
12	C^+	2.5	4.0	5.9
13	CH^+	2.3	2.0	1.3
14	CH_2^+, N^+	4.1	2.8	4.3
15	CH_3^{+a}	6.9	2.7	3.2
16	NH^+, O^+	3.5	3.5	5.2
17	NH_3^+, OH^+	2.3	1.3	1.7
18	NH_4^+, H_2O^+	3.4	3.9	3.0
19	H_3O^+	0.3	0.6	0.2
24	C_2^+	0.7	1.2	0.9
25	C_2H^+	1.2	1.0	0.5
26	$C_2H_2^+$, CN^+	2.5	1.5	1.2
27	$C_2H_3^{+a}$	3.8	1.7	1.6
28	$HCNH^{+a}$	10.2	5.9	5.7
29	NH_2CH^{+a}	3.4	1.7	2.4
30	$NH_2CH_2^{+a}$	0.3	0.3	0.4
36	C_3^+	0.2	0.3	0.2
37	C_3H^+	0.2	0.2	0.1
38	$C_3H_2^+$, C_2N^+	1.0	0.8	0.5
39	$C_3H_3^+$, C_2NH^+	0.9	0.5	0.5
40	$C_3H_4^+$, $C_2NH_2^+$	1.8	0.7	0.8
41	$C_3H_5^+$, $C_2NH_3^+$	2.1	0.6	0.7
42	$NH_2CH_2C^{+a}$	3.3	1.4	1.2
43	$NH_2CH_2CH^{+a}$	0.7	0.5	0.4
44	$NH_2CH_3CH^{+a}$	3.3	14.1	7.7
45	$HOCO^{+a}$	3.7	2.1	2.7
46	$HCOOH^+$	0.1	0.1	0.1
52		0.1	0.1	0.1
53		0.2	0.1	0.1
54		0.1	0.1	0.1
55	$C_3NH_5^+$	0.1	0.1	0.1
56			0.1	0.1
74	$NH_2CHCOOH^{+a}$	<0.1	0.2	0.1

[a]Fragment ion assignments following the work of Jochims *et al.* (Ref. 26).

TABLE II. Relative yields of the dominant cationic fragments (yield: 0.1% or more with the exception of H_3^+) of β-alanine formed in collisions with 10 keV He^+, 20 keV He^{2+}, and 50 keV O^{5+}.

m/q (amu)	Fragment ion	He^+ (%)	He^{2+} (%)	O^{5+} (%)
1	H^+	27.5	38.3	37.5
2	H_2^+	1.3	1.1	1.2
3	H_3^+	0.03	0.02	0.05
12	C^+	2.2	3.7	6.0
13	CH^+	2.3	1.7	14
14	CH^+, N^+	4.1	2.7	4.4
15	CH_3^{+a}	4.2	1.7	1.7
16	NH^+, O^+	3.5	3.8	5.3
17	NH_3^+, OH^+	2.5	1.6	2.0
18	NH_4^+, H_2O^{+a}	1.7	1.5	1.4
19	H_3O^+	0.3	0.1	0.2
24	C_2^+	1.0	1.5	1.1
25	C_2H^+	1.6	1.2	0.7
26	$C_2H_2^+$, CN_+	2.8	1.6	1.5
27	$C_2H_3^{+a}$	4.2	1.9	1.9
28	$HCNH^{+a}$	10.6	5.5	6.1
29	NH_2CH^{+a}	3.4	1.8	2.6
30	$NH_2CH_2^{+a}$	6.6	18.5	12.3
31		0.5	0.3	0.3
37	C_3H^+	0.5	0.1	0.2
38	$C_3H_2^+$, C_2N^+	1.2	0.7	0.6
39		1.1	0.4	0.6
40		1.9	0.6	0.9
41		2.4	0.7	1.0
42	$NH_2CH_2{=}C^{+,a}$ CH_2CO^+	4.3	1.8	2.2
43	$NH_2CHCH_2^{+a}$	1.3	1.5	1.2
44	$NH_2(CH_2)_2^{+a}$	1.2	1.1	1.1
45	$HOCO^{+a}$	3.5	1.7	2.5
46			0.2	0.3
50		0.2		
51		0.1		
52		0.2	0.1	0.1
53		0.3	0.1	0.1
55		0.1	0.1	0.1
60	CH_3COOH^{+a}		0.1	0.1
70	$NH_2CHCHCO^{+a}$		0.3	0.2
89	$NH_2(CH_2)_2COOH^+$	0.1	0.7	0.6

[a]Fragment ion assignments following the work of Jochims *et al.* (Ref. 26).

on fragmentation channels of the α-alanine cation find this channel to be energetically most favorable.[24]

For β-alanine, H^+ is again found to dominate the spectrum, together with the fragment at $m/q=30$ ($NH_2CH_2^+$, referred to as A in Fig. 3). The latter fragment is formed by a single rupture of the C_α–C_β bond indicated in Fig. 1. Fragment A is almost absent for α-alanine, whereas fragment B is almost absent for β-alanine. Qualitatively, the same results are observed for the other projectile ions and ion energies with the exception of He^+ projectiles, where channels A and B are less dominant. Similar findings have been reported for electron impact ionization[25] and for photoionization studies.[26]

Compared to these techniques, single electron capture from a molecule by a MCI is very selective, i.e., restrained to capture from the highest occupied molecular orbital. In the keV energy range, single electron capture also is the process with the largest cross section, dominating the fragmentation pattern in Fig. 3. As mentioned in the Introduction, single electron capture from MCI is, furthermore, known to be an extremely gentle process, accompanied only by weak excitation of the target molecule.[19,18] This is stressed by the fact that the isomer specificity of the obtained mass spectra is absent for He^+ impact (see Tables I and II) which is known to cause the most violent fragmentation in biomolecules.[9,13] For O^{5+}, the isomer specificity is weakened due to the fact that gentle single electron capture competes with gentle multielectron captures, the latter leading to a more severe fragmentation.

For a qualitative understanding of the isomer-selective fragmentation pattern, we employ the spatial spin densities of the two alanine radical cations. Overlaid on the lowest energy conformer structures, Fig. 1 shows the spatial distribution of the α- and β-alanine cation spin densities, as obtained by density functional theory calculations on the B3LYP level using a 6-311++G(d,p) basis set.[27] Since the

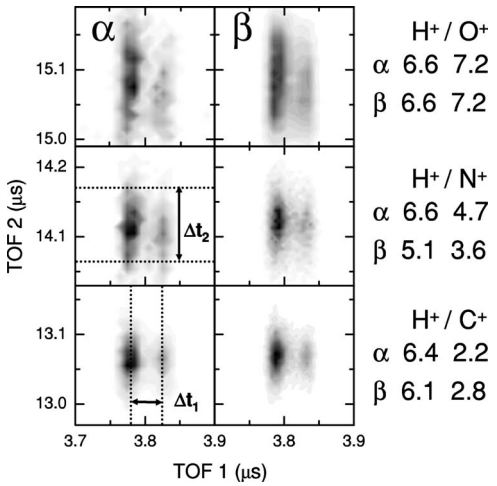

FIG. 4. Correlation plot for H^+/C^+, H^+/N^+, and H^+/O^+ ion pairs from 40 keV He^{2+} collisions with α- and β-alanine. On the right, kinetic energies are given for each fragment ion in eV (see text).

interaction time between ion and amino acids is on the femtosecond time scale, we assumed a vertical ionization. The geometries have thus been optimized for the neutral molecules. In agreement with the study of Simon *et al.*,[24] the spin density for α-alanine is centered around the NH_2 (amino) group. We find similar results for β-alanine. In both cases, weaker contributions of spin density are also found on the respective COOH groups. However, for α-alanine where the amino group is bound to the central C atom, the ionization substantially weakens the $C–C_\alpha$ bond, whereas for β-alanine, the C_α–C bond is weakened (see Fig. 1). This is in agreement with the experimental data in which scission of these bonds is preferentially observed.

Fragmentation patterns as the ones shown in Fig. 3 mostly contain information on possible endpoints of the ion induced dissociation processes as well as on their respective branching ratios. When only examining those ionization processes in which the alanine molecules are at least doubly ionized, two or more fragment cations stemming from the same molecular fragmentation event can be detected in coincidence and more in depth information on the fragmentation dynamics can be obtained. In the following, we will focus on the analysis of those fragmentation channels that involve the most abundant fragment ions from Fig. 3, i.e., $NH_2CH_3CH^+$ (α-alanine), $NH_2CH_2^+$ (β-alanine), and H^+ (both).

Fragment-fragment correlations involving protons are dominating the correlation diagrams for both isomers. Furthermore, protons are often the most energetic secondary ions observed in ion induced biomolecular fragmentation.[9] Figure 4 exemplarily displays the correlation plots for H^+ (TOF1) with C^+, N^+, and O^+ (TOF2) formed after multiple ionization of α- and β-alanine by 40 keV He^{2+} ion impact. Note that the double-island structure is due to the transmission of the extraction system. In the collision center, fragment ions with a specific kinetic energy are produced. The static electric extraction field applied to the collison region accelerated the ions toward a diaphragm of finite diameter. Depending on the diaphragm diameter, its distance from the collision center and the strength of the extraction field, a cutoff ion energy exists. Ions with kinetic energies exceeding this cutoff energy have transmissions smaller than 100%. For a single ion, the transmission depends on the ion momentum vector. If the angle between the ion momentum and detector axis is 90°, the ion will reach the diaphragm at a maximum distance from the center. If this angle is zero, the ion will reach the diaphragm at the diaphragm center. For fragment ions with kinetic energies exceeding the cutoff, therefore only the ones emitted parallel or antiparallel to the spectrometer axis are detected. In case of 100% transmission, parallelogram-shaped islands would be observed. In Fig. 4 for the protons, a structure with two maxima is observed and Δt_1 is defined as the distance between these maxima. For the heavy ions, no double peak structure is observed. As a measure for their kinetic energies, we use the time (Δt_2) between those TOFs at which the peak intensity dropped to 10%. For a given extraction field ε, fragment charge state q, and fragment ion mass m, the ion kinetic energy is given by $E = \varepsilon^2 q^2 \Delta t^2 / 8m$. The determined energies for fragments of α- and β-alanine are given on the right of Fig. 4 (in eV).

It is obvious that the fragment ion kinetic energies depend strongly on the fragment ion type, being largest for O^+ and H^+ and smallest for C^+. The isomer dependence is relatively weak. For O^{5+} projectiles, qualitatively the same trends are observed but, since, on average fragmentation involves higher initial alanine charge states, fragment kinetic energies exceed 15 eV (H^+, most probable energy) and 17 eV (O^+, energy at 10% cutoff). On the other hand, for He^+ ions for which resonant electron capture is unlikely,[8] a strong isomer dependence is observed.

In the case of double ionization of α-alanine, the dominating large fragment $NH_2CH_3CH^+$ formed by scission of the $C–C_\alpha$ bond is not seen as a strong fragmentation channel in the correlation data. Apparently, two electron removal quenches this fragment and leads to a more extensive fragmentation of this ion. Somewhat weak, but as the most intense feature at larger fragment masses, we observe the corresponding $COOH^+$ fragment at $m/q=45$ which is only a minor channel in single ionization (see Table I). The relevant parts of the respective correlation plots are displayed in Fig. 5. The $COOH^+$ ion is observed strongest in coincidence with the NH_2CH^+ ion ($m/q=29$) and to a weaker extent with $HCNH^+$ ($m/q=28$) and HCN^+ ($m/q=27$); note that Jochims *et al.*[26] assigned this m/q to $C_2H_3^+$. Our results indicate that the three m/q differ in hydrogen content, favoring the HCN^+ assignment. A second group of islands represents coincidences of $COOH^+$ with CH_3^+ ($m/q=15$) and NH_4^+ ($m/q=18$).

The slope of islands in TOF/TOF correlation plots carries information on the momentum balance of the respective fragment ions. If the two ions stem from a two-body breakup, conservation of momentum implies a −1 slope of the respective island in the correlation plot. Nonconservation of mass obviously rules out two-body breakup and a two-step process has to be invoked.

In Fig. 5, the islands have a much steeper slope, indicating a secondary decay mechanism[28] subsequent to the first step in which the $C–C_\alpha$ bond is broken. In the second step,

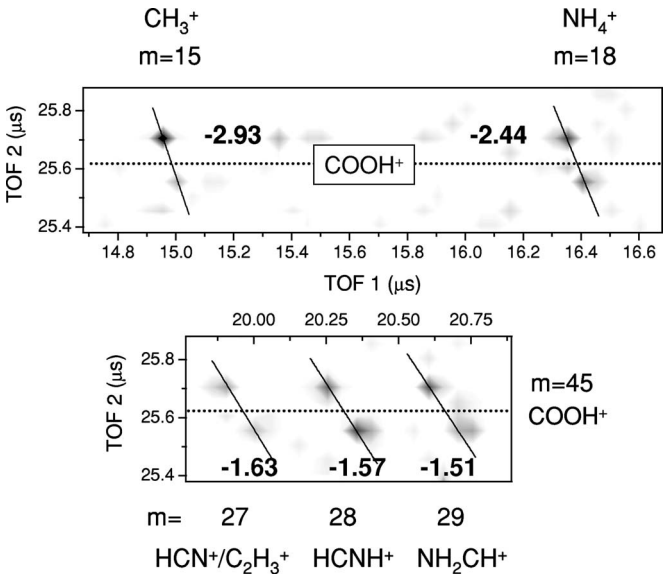

FIG. 5. Correlation plot for fragment ions from 40 keV He^{2+} collisions with α-alanine with intensities given in logarithmic scale. Only the regions corresponding to $m/q=15$–18 and $m/q=27$–29 coincidences with $COOH^+$ are shown, with the number indicating the respective island slope.

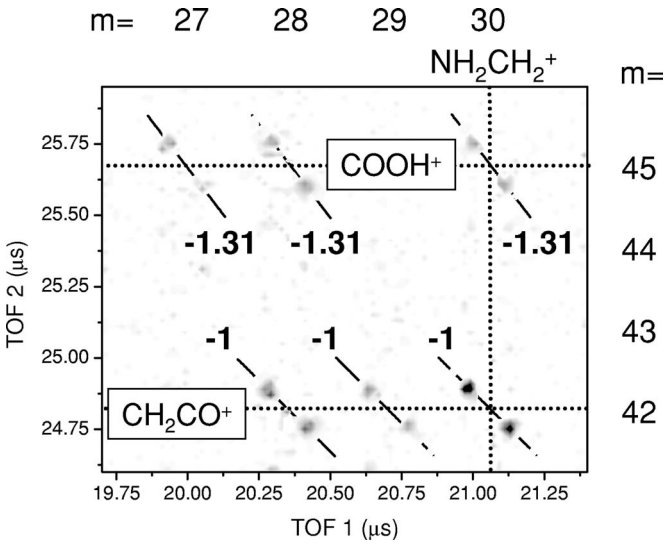

FIG. 6. Correlation plot for fragment ions from 40 keV He^{2+} collisions with β-alanine with intensities given in logarithmic scale. Only the region corresponding to $NH_2CH_2^+(-H_n)$ (due to cleavage of the C_α–C_β bond) coincidences with $COOH^+$ (due to cleavage of the C–C_α bond) and CH_2CO^+ (due to cleavage of the C–O single bond) are shown, with the number indicating the respective island slope.

the $NH_2CH_3CH^+$ ion fragments, e.g., along the C_α–C_β bond [pair (45,29)] according to the following scheme:

$$NH_2CH_2CH_2COOH^{++} \rightarrow NH_2CH_3CH^+ + COOH^+, \quad (1)$$

$$\rightarrow NH_2CH^+ + CH_3 + COOH^+. \quad (2)$$

If no kinetic energy is released in the second step, then the NH_2CH^+ cation leaves with the same velocity as the initial $NH_2CH_3CH^+$ cation. The slope of the island has to be $-m(NH_2CH_3CH^+)/m(NH_2CH^+)=-44/29=-1.51$, which is in line with the experimental data (see Fig. 5). A similar fragmentation sequence leads to the pairs (45,28) (slope=−1.57) and (45,27) (slope=−1.63) in which either one or two hydrogen atoms are lost in the second step. In case the charge stays on the smaller CH_3 fragment, the pair (45,15) (slope=−2.93) is observed. The last channel seen in Fig. 5 corresponding to the pair (45,18) (slope=−2.44) leads to the formation of an NH_4^+ ion. This channel involves rearrangement of the $NH_2CH_3CH^+$ cation.[25]

The kinetic energy release in step 1 amounts to 2.2 ± 0.2 eV [pair (30,45)]. In the single-stop spectra (Fig. 3), the dominating fragment cation for β-alanine is $NH_2CH_2^+$ ($m/q=30$). In the coincidence spectra (Fig. 6), the strongest correlation of $m/q=30$ is with $m/q=42$ (CH_2CO^+). Loss of one or two H atoms from $NH_2CH_2^+$ leads to pairs (29,42) and (28,42). All these islands have a slope very close to −1.

The three pairs (28,42), (29,42), and (30,42) are obviously not the result of a pure two-body breakup because a neutral OH fragment is produced in addition. Since two-body breakup is ruled out, the −1 slope is an indication for the so-called deferred charge separation,[28] i.e., loss of a neutral fragment without appreciable energy release [Eq. (1)] and subsequent fragmentation of the remaining dication under conservation of momentum [Eq. (2)],

$$NH_2CH_2CH_2COOH^{++} \rightarrow NH_2CH_2CH_2CO^{++} + OH, \quad (3)$$

$$\rightarrow NH_2CH_2^+ + CH_2CO^+ + OH. \quad (4)$$

The kinetic energy released in the second step can be obtained from the Δt of the respective island and amounts to 3.5 ± 0.2 eV for the fragmention into pair (30,42). A weaker group of islands involving the most prominent $NH_2CH_2^+$ ($m/q=30$) cation is due to correlations with $m/q=45$ ($COOH^+$). This channel is also observed accompanied by loss of two or three H atoms from the lighter fragment, leading to pairs (28,45) and (27,45). Here, the islands have a much steeper slope, indicating a secondary decay mechanism,[28]

$$NH_2CH_2CH_2COOH^{++} \rightarrow NH_2CH_2^+ + CH_2COOH^+, \quad (5)$$

$$\rightarrow NH_2CH_2^+ + COOH^+ + CH_2. \quad (6)$$

Again, if no kinetic energy is released in the second step, then the $COOH^+$ cation leaves with the same velocity as the initial CH_2COOH^+ cation. The slope of the islands has to be $-m(CH_2COOH)/m(COOH)=-59/45=-1.31$, which agrees very well with what is observed in Fig. 6. The kinetic energy release in step 1 amounts to 2.2 ± 0.2 eV [pair (30,45)]. This value is clearly smaller than the 3.5 eV observed for the competing process. The reason might be that the charge separation occurs in the first step, i.e., from the intact molecule. In the deferred charged separation process, the intact molecule has already lost an OH group. Coulomb explosion then occurs in a smaller system where the distances are smaller and Coulomb repulsion is accordingly stronger.

The fragmentation dynamics following alanine double ionization can be interpreted by looking at the electron den-

sity difference maps for dication and cation (see Fig. 1). The major bond scission following single ionization is marked by black lines. Subsequent bond scissions in the case of double ionization are marked by gray (red) lines.

For α-alanine, the main fragmentation process after single ionization is the scission of the C–C_α bond, leading to a neutral COOH fragment. This is also the most common first step after double ionization [see Eq. (2)] with the only difference of COOH being formed in cationic form. From Fig. 1, this can be expected since substantial charge is removed from the COOH group upon the second ionization. Furthermore, the CH_3 group is again only weakly affected by removal of the second electron. It is this group which is set free in the second step, either neutral or in cationic form.

Formation of the $COOH^+$ cation is also an important channel in double ionization of β-alanine [see Eq. (6)]. It is obvious from the electron density difference maps in Fig. 1 that electron removal from the β-alanine cation changes the electron density throughout the whole molecule. In particular, the C–C_α bond is affected and in the case of the C–C_α bond scission, the $COOH^+$ is released in the second fragmentation step.

A peculiarity of the β isomer is the OH-loss channel [Eq. (4)] which is stronger than the $COOH^+$ production. Here, the *first* step is the scission of the C–O single bond (indicated by dotted lines in Fig. 1) followed by scission of the C_α–C_β bond. This process is probably facilitated by a stronger intramolecular hydrogen bonding between the NH_2 group and the second O atom.

CONCLUSION

To conclude, we have observed a pronounced isomer dependence in MCI induced fragmentation of isolated alanine molecules. These results are interesting for future studies on MCI induced protein fragmentation with the ultimate goal of developing a new complementary tool for protein structure determination. Fragment ion kinetic energies were found to exceed 6 eV (He^{2+} impact) and 15 eV (O^{5+} impact), implying that ion induced damage of histone proteins might produce sufficiently energetic secondary ions to induce further damage to neighboring DNA. Formation of H_3^+ ions from both α- and β-alanine was observed. This relatively weak process requires substantial rearrangement of the molecule before fragmentation. Thus, formation of H_3^+ cations in MCI induced fragmentation, as first observed by De *et al.*,[20] seems to be a more general phenomenon, which is also observed in biomolecular fragmentation.

ACKNOWLEDGMENTS

This experiment has been performed at the ZERNIKELEIF part of the distributed LEIF infrastructure. The support received by the European Project ITS LEIF (RII3/026015) is gratefully acknowledged. Financial support from the Stichting voor Fundamenteel Onderzoek der Materie (FOM) which is supported by the Nederlandse Organisatie voor Wetenschapelijk Onderzoek (NWO) is gratefully acknowledged. P.S. acknowledges financial support from European Marie Curie Fellowship program, Contract No. 350470.

[1] M. A. Huels, I. Hahndorf, E. Illenberger, and L. Sanche, J. Chem. Phys. **108**, 1309 (1998).
[2] H. Abdoul-Carime, M. A. Huels, F. Brüning, E. Illenberger, and L. Sanche, J. Chem. Phys. **113**, 2517 (2000).
[3] G. Hanel, B. Gstir, S. Denifl, P. Scheier, M. Probst, B. Farizon, M. Farizon, E. Illenberger, and T. D. Märk, Phys. Rev. Lett. **90**, 188104 (2003).
[4] S. Ptasinska, S. Denifl, P. Scheier, and T. D. Märk, J. Chem. Phys. **120**, 8505 (2004).
[5] B. Boudaïffa, P. Cloutier, D. Hunting, M. A. Huels, and L. Sanche, Science **287**, 1658 (2000).
[6] X. Pan, C. Cloutier, D. Hunting, and L. Sanche, Phys. Rev. Lett. **90**, 208102 (2003).
[7] F. Martin, P. D. Burrow, Z. Cai, P. Cloutier, D. Hunting, and L. Sanche, Phys. Rev. Lett. **93**, 068101 (2004).
[8] J. de Vries, R. Hoekstra, R. Morgenstern, and T. Schlathölter, J. Phys. B **35**, 4373 (2002).
[9] J. de Vries, R. Hoekstra, R. Morgenstern, and T. Schlathölter, Eur. Phys. J. D **24**, 161 (2003).
[10] J. de Vries, R. Hoekstra, R. Morgenstern, and T. Schlathölter, Phys. Rev. Lett. **91**, 053401 (2003).
[11] R. Brédy, J. Bernard, L. Chen, B. Wei, A. Salmoun, T. Bouchama, M. C. Buchet-Poulizac, and S. Martin, Nucl. Instrum. Methods Phys. Res. B **235**, 392 (2005).
[12] T. Schlathölter, F. Alvarado, S. Bari, A. Lecointre, R. Hoekstra, V. Bernigaud, B. Manil, J. Rangama, and B. Huber, ChemPhysChem **7**, 2339 (2006).
[13] F. Alvarado, S. Bari, R. Hoekstra, and T. Schlathölter, Phys. Chem. Chem. Phys. **8**, 1922 (2006).
[14] Z. Deng, I. Bald, E. Illenberger, and M. A. Huels, Phys. Rev. Lett. **95**, 153201 (2005).
[15] Z. Deng, I. Bald, E. Illenberger, and M. A. Huels, Phys. Rev. Lett. **96**, 243203 (2006).
[16] S. Blanco, A. Lesarri, J. C. Lopez, and J. L. Alonso, J. Am. Chem. Soc. **126**, 11675 (2004).
[17] M. E. Sanz, A. Lesarri, M. I. Pena, V. Vaquero, V. Cortijo, J. C. Lopez, and J. L. Alonso, J. Am. Chem. Soc. **128**, 3812 (2006).
[18] B. Walch, C. L. Cocke, R. Voelpel, and E. Salzborn, Phys. Rev. Lett. **72**, 1439 (1994).
[19] T. Schlathölter, O. Hadjar, R. Hoekstra, and R. Morgenstern, Appl. Phys. A: Mater. Sci. Process. **72**, 281 (2001).
[20] S. De, J. Rajput, A. Roy, P. N. Ghosh, and C. P. Safvan, Phys. Rev. Lett. **97**, 213201 (2006).
[21] O. Hadjar, R. Hoekstra, R. Morgenstern, and T. Schlathölter, Phys. Rev. A **63**, 033201 (2001).
[22] I. Ipolyi, P. Cicmand, S. Denifl, V. Matejcik, P. Mach, J. Urban, P. Scheier, T. D. Mark, and S. Matejcik, Int. J. Mass. Spectrom. **252**, 228 (2006).
[23] M. Morita, M. Mori, T. Sunami, H. Yoshida, and A. Hiraya, Chem. Phys. Lett. **417**, 246 (2006).
[24] S. Simon, A. Gilb, M. Sodupeb, and J. Bertran, J. Mol. Struct.: THEOCHEM **727**, 191 (2005).
[25] G. Junk and H. Svec, J. Am. Chem. Soc. **85**, 839 (1963).
[26] H.-W. Jochims, M. Schwell, J.-L. Chotin, M. Clemino, F. Dulieu, H. Baumgärtel, and S. Leach, Chem. Phys. **298**, 279 (2004).
[27] M. J. Frisch M. J. Trucks, G. W. Schlegel *et al.*, GAUSSIAN 03, Revision C.02. Gaussian, Inc., Wallingford, CT, 2004.
[28] J. H. D. Eland, F. S. Wort, and R. N. Royds, J. Electron Spectrosc. Relat. Phenom. **41**, 297 (1986).